Industrial Chemistry & Materials

ROYAL SOCIETY OF CHEMISTRY

PAPER

View Article Online
View Journal | View Issue

Cite this: *Ind. Chem. Mater.*, 2025, **3**, 744

Improved CO_2 capture performance of CeO_2-doped CaO-based pellets: effects of particle size and steam treatment†

Yong Li,[a] Wuhao Sun,[a] Xilei Liu,[a] Jian Chen, *[a] Hedan Tang,[a] Youshi Li,[a] Mingdi Li [a] and Lunbo Duan *[b]

Rapid deactivation of CaO-based sorbents remains a major challenge for the calcium looping (CaL) process. Recently, CeO_2, known for its high Tammann temperature and abundant oxygen vacancies, has been extensively investigated for CaO-based sorbents to mitigate performance degradation. In this study, CeO_2-doped CaO-based pellets, prepared in a more industrially relevant form for the first time, were investigated. The incorporation of CeO_2 alleviated the negative impact of pelletization and particle size on performance. CeO_2-doped CaO-based pellets with different particle sizes (106–180, 180–250, 250–355, and 355–500 μm) exhibited nearly identical CO_2 capture performance, closely matching the reactivity of powdery CeO_2-doped CaO-based sorbents. Furthermore, the effects of two steam-based strategies—steam hydration and steam injection—on the reactivity of the CeO_2-doped pellets were explored. Hydration after the sixth calcination significantly enhanced the reactivity of CeO_2-doped CaO-based pellets. Hydration at 650 °C resulted in a conversion of 86.0% at the sixth cycle, surpassing the non-hydrated pellets by 55.4%. In contrast, steam hydration had minimal impact on the performance of undoped CaO-based pellets, indicating that CeO_2 greatly enhanced the improvement from steam hydration. The effect of steam injection was more complex and highly dependent on the steam concentration. Only a moderate steam concentration (10–15%) enhanced the reactivity, leading to higher carbonation conversions. With 10% steam during carbonation, the initial conversion surged to 93.8%, representing a 22.0% improvement over the counterpart without steam.

Received 27th January 2025,
Accepted 8th April 2025

DOI: 10.1039/d5im00017c

rsc.li/icm

Keywords: CO_2 capture; Calcium looping (CaL); Stabilizer; Oxygen vacancy; Particle size; Steam.

1 Introduction

The calcium looping (CaL) process, which relies on the reversible carbonation/calcination reaction between CO_2 and CaO-based sorbents, stands out as a highly effective method for reducing anthropogenic CO_2 emissions.[1–3] As depicted in Fig. 1, the carbonation reaction takes place in a carbonator, where CO_2 from flue gas (*e.g.*, emitted by coal-fired power plants) reacts with CaO to form $CaCO_3$ (reaction 1). The produced $CaCO_3$ is then moved to a calciner, where it is heated to high temperatures, regenerating CaO and releasing CO_2 (reaction 2). Oxyfuel combustion is often employed in calciners, which helps produce a concentrated CO_2 stream at the outlet.[4,5] CaO-based sorbents are an attractive option for CO_2 capture due to their abundant availability, high theoretical CO_2 uptake (~786 g_{CO_2} kg_{CaO}^{-1}), and cost-effectiveness. As a result, substantial research has been focused on advancing the CaL process to make it more commercially viable.[6,7] However, a significant challenge remains: the rapid performance decay of CaO-based sorbents.[8] Consequently, enhancing the reactivity and stability of sorbents has become a central research focus.

$$CaO + CO_2 \rightarrow CaCO_3 \quad \Delta H = -178\ kJ\ mol^{-1} \qquad \text{(Reaction 1)}$$

$$CaCO_3 + CaO \rightarrow CO_2 \quad \Delta H = +178\ kJ\ mol^{-1} \qquad \text{(Reaction 2)}$$

An alternative approach to improve the performance of sorbents is the doping of additives.[9,10] Different inert stabilizers (*e.g.*, Al_2O_3,[11] ZrO_2,[12] MgO,[13] Y_2O_3,[14] and SiO_2[15]) and active promoters (*e.g.*, Na_2CO_3,[16] KCl,[17] and K_2CO_3[18]) have been investigated as additives for CaO-based sorbents. Recent studies show that the carbonation process itself involves three subreactions: CO_2 adsorption, surface reaction with O^{2-} to CO_3^{2-}, and $CaCO_3$ production (reactions 3–5).

[a] *School of Automotive Engineering, Changshu Institute of Technology, Changshu 215500, China. E-mail: chenjian@cslg.edu.cn*
[b] *Key Laboratory of Energy Thermal Conversion and Control, Ministry of Education, School of Energy and Environment, Southeast University, Nanjing 210096, China. E-mail: duanlunbo@seu.edu.cn*

† Electronic supplementary information (ESI) available. See DOI: https://doi.org/10.1039/d5im00017c

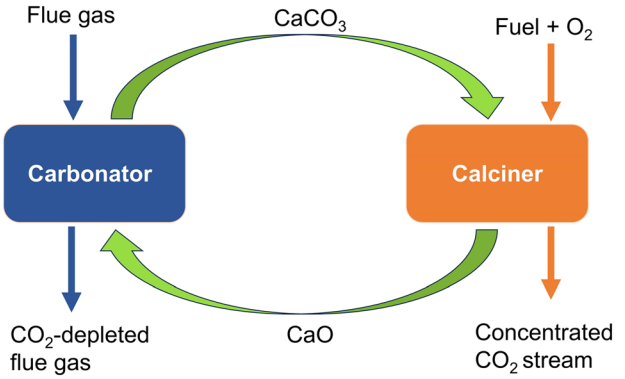

Fig. 1 Illustration of the CaL technology for capturing CO_2 from the flue gas.

The diffusion of CO_2 and mobility of O^{2-} are critical factors influencing the rate and efficiency of the carbonation reaction.[19] A density functional theory study confirmed that oxygen vacancies facilitated the diffusion of CO_2.[19] Yi *et al.* added oxygen vacancy-containing additives ($Ce_xZr_{1-x}O_2$ and $LaAl_yMg_{1-y}O_3$) into CaO-based sorbents, and found that CO_2 capture stability was directly related to the presence of oxygen vacancies in the additives.[20] These results underscored the potential for enhancing the reactivity of CaO-based sorbents by introducing oxygen vacancies.[19,21]

CeO_2 has emerged as an excellent candidate for doping into CaO-based sorbents. It has a high Tammann temperature of 1064 °C[22] and abundant oxygen vacancies from the coexistence of Ce^{3+} and Ce^{4+}.[23] The oxygen vacancies are essential for promoting the carbonation reaction, potentially resulting in improved CO_2 capture ability.[21] Research demonstrated that adding CeO_2 to CaO-based sorbents boosted the number of oxygen vacancies, promoting CO_2 sorption.[24,25] Yanase *et al.* observed a decrease in the activation energy of the carbonation reaction from 107 to 41 kJ mol^{-1} when the CeO_2/CaO mass ratio increased from 0 to 2, confirming the promotion effect of CeO_2.[26] Similarly, Wang *et al.* claimed that adding CeO_2 accelerated the carbonation reaction rate and increased the CO_2 uptake capacity within a short reaction duration.[22] Furthermore, several researchers, including Liu *et al.*,[24] Jiang *et al.*,[25] Yan *et al.*,[27] and Guo *et al.*,[28] prepared CeO_2-doped CaO-based sorbents using various synthesis approaches. These studies all confirmed the beneficial role of CeO_2 in enhancing sorbent reactivity, primarily attributed to the presence of oxygen vacancies, as verified by X-ray photoelectron spectroscopy (XPS) analysis. However, it is important to note that these studies mainly focused on the preparation and evaluation of powdery sorbents.

$$CO_2(g) \leftrightarrow CO_2(ads) \quad \text{(Reaction 3)}$$

$$CO_2(ads) + O^{2-} \rightarrow CO_3^{2-} \quad \text{(Reaction 4)}$$

$$CO_3^{2-} + CaO \rightarrow CaCO_3 + O^{2-} \quad \text{(Reaction 5)}$$

In addition, using steam is an effective method for enhancing the reactivity of CaO-based sorbents.[29] Steam can be introduced into the system through two primary strategies: (i) adjusting the steam concentration in the carbonator and (ii) introducing an external reactor between the calciner and carbonator, where steam hydration takes place (reaction 6). The first approach takes advantage of the steam naturally present in flue gas, which typically contains steam concentrations ranging from 5% to 20%.[30] For instance, Manovic *et al.* found that introducing 15% steam during carbonation significantly increased the CO_2 uptake capacity, achieving 0.33 g_{CO_2} $g_{sorbent}^{-1}$ after ten cycles.[31] This was 120% higher than the capacity achieved in the counterpart without steam. The second approach involves the use of an external reactor to hydrate the spent sorbents, thus recovering their performance. Yu *et al.* reported that after hydration, the capacity of spent pellets boosted from 0.11 to 0.42 g_{CO_2} $g_{sorbent}^{-1}$.[32] This improvement is attributed to the higher molar volume of $Ca(OH)_2$ (~33.7 cm^3 mol^{-1}) compared to CaO (~16.9 cm^3 mol^{-1}).[33] The formation of $Ca(OH)_2$ leads to particle expansion and surface cracking, ultimately increasing the porosity.[34]

$$CaO + H_2O \rightarrow Ca(OH)_2 \quad \Delta H = -109 \text{ kJ mol}^{-1} \quad \text{(Reaction 6)}$$

Fluidized bed reactors are often recommended for industrial applications of the CaL process, necessitating the use of CaO-based sorbents in pellet form.[35,36] However, most recent studies have primarily focused on developing powdery CeO_2-doped CaO-based sorbents, followed by evaluations of their cyclic performance.[22,24,25,37] Nevertheless, using pelletized sorbents in the CaL process is crucial for practical applications. Therefore, in this study, CeO_2-doped CaO-based pellets with varying particle sizes were prepared for the first time, aiming to investigate their performance in a more industrially relevant form. Additionally, the impacts of two steam-based strategies—steam hydration and steam injection—on the performance of these pellets were explored. These methods were tested to assess their potential for enhancing the cyclic reactivity of pelletized sorbents in the context of the CaL process.

2 Results and discussion

2.1 Effect of CeO_2 content on the reactivity of powdery CeO_2-doped CaO-based sorbents

A series of CaO-based sorbents doped with varying CeO_2 contents were prepared using the Pechini technique. The crystalline phase compositions of the resulting sorbents were characterized by XRD, and the results are shown in Fig. 2a. For the undoped CaO-based sorbent (*i.e.*, CaO-PO), the XRD pattern revealed the presence of only the CaO crystalline phase, indicating the successful synthesis of pure calcium oxide. Upon doping with CeO_2, the XRD patterns of the CeO_2-doped CaO-based sorbents showed two distinct crystalline phases: CaO and CeO_2. The intensity of the CeO_2 peaks

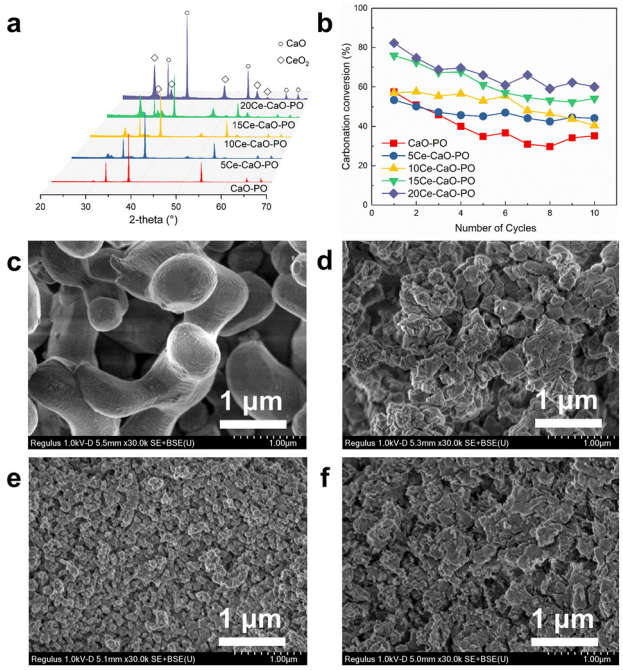

Fig. 2 Characterization and reactivity of powdery CeO_2-doped CaO-based sorbents. (a) XRD patterns of fresh samples; (b) CO_2 capture performance of CeO_2-doped CaO-based sorbents over multiple carbonation/calcination cycles in a dual-packed bed reactor. A higher CeO_2 content improves CO_2 uptake retention and reduces performance decay; SEM images of (c) fresh CaO-PO, (d) spent CaO-PO, (e) fresh 20Ce-CaO-PO, and (f) spent 20Ce-CaO-PO. CeO_2 effectively reduces the grain size and reduces the sintering of sorbents during cycling. Reaction conditions: calcination: N_2, 850 °C, 10 min; carbonation: 15% CO_2, 85% N_2, 650 °C, 15 min.

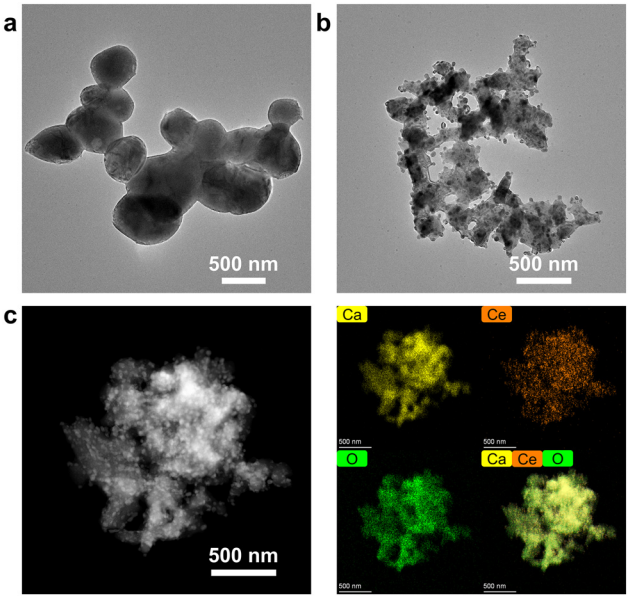

Fig. 3 HAADF-STEM images and EDX mapping of fresh CaO-PO and 20Ce-CaO-PO. (a) HAADF-STEM image of CaO-PO; (b) HAADF-STEM image and (c) EDX mapping of 20Ce-CaO-PO. CeO_2 effectively reduces the grain size.

increased as the CeO_2 content increased. Additionally, ICP-OES measurements were conducted to quantify the exact CeO_2 content incorporated into the sorbents. The ICP-OES analysis revealed that the actual mass ratio of CeO_2 to CaO matched the theoretical values, validating the precision of the doping process.

Fig. 2b shows the performance of the undoped sorbent and those doped with different CeO_2 contents over ten testing cycles. The undoped CaO-based sorbent, CaO-PO, demonstrated an initial conversion of 57.5%, dropping to 35.2% in the tenth cycle and corresponding to a reactivity loss of 38.8%. In contrast, the addition of 5 wt% CeO_2 resulted in a slightly lower initial carbonation conversion for 5Ce-CaO-PO (~53.4%) compared to CaO-PO (~57.5%). Nevertheless, 5Ce-CaO-PO retained a conversion of 44.2% after ten cycles, maintaining 82.7% of the original performance and exceeding CaO-PO by 30%. Increasing the CeO_2 content to 10 wt% yielded 10Ce-CaO-PO with initial and final carbonation conversions of 57.1% and 40.4%, respectively. When the CeO_2 content reached 15 wt%, 15Ce-CaO-PO achieved an initial carbonation conversion of 75.9%, 30% higher than that of CaO-PO. It retained a conversion of 54.2% after ten cycles, outperforming CaO-PO by 50%. At 20 wt% CeO_2 doping, 20Ce-CaO-PO exhibited the highest initial carbonation conversion of 82.3%, which decreased to 60.1% after ten cycles, preserving 73% of its original reactivity. Given the high cost of the CeO_2 precursor, the optimal CeO_2 content was found to be 20 wt%, which provided high CO_2 uptake capacity and excellent cyclic stability. In addition, the CO_2 capture experiments conducted in the vertical fixed bed reactor revealed that CeO_2 doping significantly enhanced the CO_2 sorption rate during carbonation (Fig. S1†).

SEM and TEM images of fresh CaO-PO and 20Ce-CaO-PO revealed that CeO_2 doping effectively reduced the grain size of the sorbents, as shown in Fig. 2c and e and 3a and b. Incorporating CeO_2 into the CaO-based sorbents resulted in a more refined microstructure, contributing to improved structural stability. A homogeneous distribution of Ca, Ce, and O elements was also observed in the fresh 20Ce-CaO-PO, confirming the uniform dispersion of CeO_2 throughout the material. This homogeneous elemental distribution was crucial as it enabled CeO_2 to function as a structural framework. After ten cycles, the spent 20Ce-CaO-PO exhibited less sintering than the spent CaO-PO, as demonstrated in Fig. 2d and f. This observation suggested that CeO_2 doping played a significant role in mitigating sintering during cyclic operations.

In addition, XPS characterization was performed to further investigate the surface properties of fresh 20Ce-CaO-PO. As shown in Fig. 4a, six distinct peaks appeared in the Ce 3d spectra, which corresponded to both Ce^{3+} and Ce^{4+}. According to the charge balance principle, the formation of oxygen vacancies was typically accompanied by the reduction of Ce^{4+} to Ce^{3+}.[38] Therefore, the presence of Ce^{3+} in the spectrum provided direct evidence for the formation of oxygen vacancies within the sorbent. Moreover, two distinct

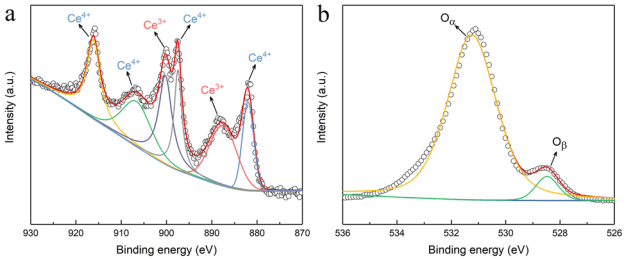

Fig. 4 XPS spectra of fresh 20Ce-CaO-PO. (a) Ce 3d and (b) O 1s.

peaks were observed in the O 1s spectra (Fig. 4b). The peak at 531.2 eV was associated with surface-adsorbed oxygen species (*i.e.*, O_α), while that present at 528.5 eV was related to lattice oxygen species (*i.e.*, O_β). Oxygen vacancies were closely associated with the O_α species, as these vacancies increased the concentration of O_α species on the surface.[38,39] The $O_\alpha/(O_\alpha + O_\beta)$ ratio, which was found to be 94%, indicated a high concentration of oxygen vacancies.

2.2 Effect of particle size on the reactivity of CeO_2-doped CaO-based pellets

The most effective powdery sorbent, *i.e.*, 20Ce-CaO-PO, was used to prepare pellets with varying particle sizes, including 106–180, 180–250, 250–355, and 355–500 μm. These pellets were then subjected to cyclic experiments to assess their reactivity over multiple cycles. As presented in Fig. 5, after the pelletization process, a slight reduction in reactivity was observed for all CeO_2-doped CaO-based pellets compared to the powdery form. Specifically, 20Ce-CaO-PE-1, which had a particle size range of 106–180 μm, exhibited an initial carbonation conversion of 79.3%, which was close to that of 20Ce-CaO-PO (~82.3%). By the tenth cycle, the reactivity of 20Ce-CaO-PE-1 decreased to 51.0%, retaining 64.4% of its initial reactivity. This represented a decrease of 15.1% in comparison to the reactivity of 20Ce-CaO-PO.

Interestingly, particle size had minimal impact on the performance of CeO_2-doped CaO-based pellets. For instance, 20Ce-CaO-PE-4, with a larger particle size range of 355–500 μm, showed initial and final carbonation conversions of 76.9% and 50.6%, respectively. These values were nearly identical to those of 20Ce-CaO-PE-1, suggesting that the particle size did not significantly influence the carbonation performance. This finding aligned with the results from previous studies.[40–44] The negligible impact of particle size on carbonation performance can be attributed to the slight reduction in the specific surface area and pore volume as the particle size increased, as detailed in Table S1.† Moreover, when comparing Fig. 6, it was evident that all CeO_2-doped CaO-based pellets maintained higher porosity than their undoped counterparts after repeated cycles. This finding is especially important for industrial applications of CeO_2-doped pellets in fluidized bed systems, where particle size effects on reactivity are common concerns.[40]

As previously mentioned, oxyfuel combustion is often recommended to produce a concentrated CO_2 stream at the calciner outlet. However, the occurrence of the calcination reaction in a CO_2-rich atmosphere increases the calcination temperature and accelerates material sintering. In recent years, O_2/H_2O combustion has been performed in calciners to reduce the calcination temperature by lowering CO_2 concentration. Therefore, the reactivity of 20Ce-CaO-PE-4 was further assessed under these industrially relevant calcination conditions. As shown in Fig. 7, when calcination was performed at 920 °C in CO_2, the reactivity of 20Ce-CaO-PE-4 dropped significantly. It had a final conversion of 25.8% by the tenth cycle, about 50% of the N_2 counterpart. In contrast, when calcination was performed at 850 °C in steam, 20Ce-CaO-PE-4 demonstrated a moderate performance decline. It had an initial carbonation conversion of 75.1%, which dropped to 29.9% by the 20th cycle, retaining 40% of the original performance. These results suggested that the O_2/H_2O combustion method offered significant advantages in reducing the calcination temperature while maintaining relatively stable performance. Table S2† summarizes the carbonation performance of the CaO-based pellets prepared in this study and those reported previously. As shown in Table S2,† 20Ce-CaO-PE-4 exhibited competitive carbonation

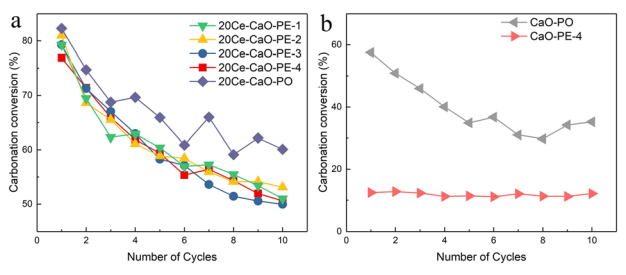

Fig. 5 Reactivity of the (a) CeO_2-doped and (b) undoped CaO-based pellets sieved to different particle sizes in the dual-packed bed reactor. Particle size had minimal impact on the performance of CeO_2-doped CaO-based pellets. Reaction conditions: calcination: N_2, 850 °C, 10 min; carbonation: 15% CO_2, 85% N_2, 650 °C, 15 min.

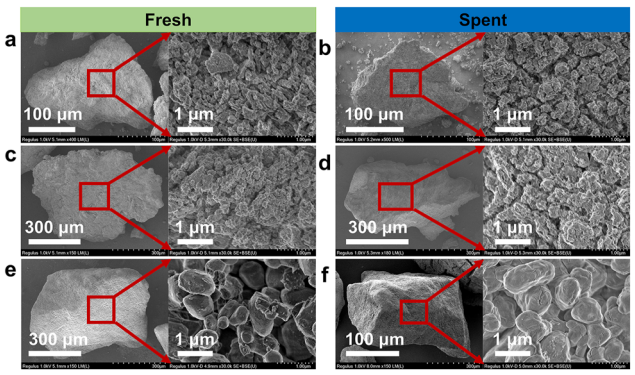

Fig. 6 SEM images of the CeO_2-doped and undoped CaO-based pellets before and after ten cycles measured in the dual-packed bed reactor. (a) Fresh and (b) spent 20Ce-CaO-PE-1; (c) fresh and (d) spent 20Ce-CaO-PE-4; (e) fresh and (f) spent CaO-PE-4.

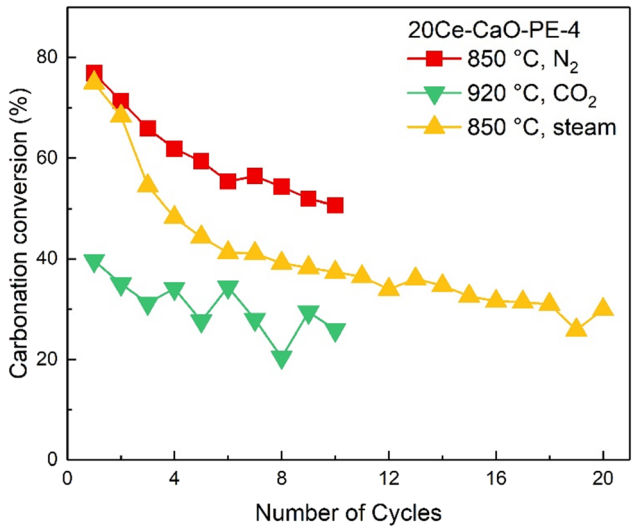

Fig. 7 Reactivity of 20Ce-CaO-PE-4 under different calcination conditions in the dual-packed bed reactor. Reaction conditions: calcination: 10 min; carbonation: 15% CO_2, 85% N_2, 650 °C, 15 min.

performance, making it a promising candidate for industrial applications.

2.3 Effect of steam hydration on the reactivity of CeO_2-doped CaO-based pellets

To enhance the CO_2 capture performance of CeO_2-doped CaO-based pellets, a steam hydration strategy was employed following the sixth calcination. The pellets were subjected to steam treatment in an external hydrator to investigate how hydration affected their reactivity. The reactivity of these hydrated pellets at different temperatures was then evaluated, with results shown in Fig. 8. Since the decomposition of $Ca(OH)_2$ starts at approximately 420 °C,[34] the hydration process was primarily conducted at 120–400 °C. Hydration at 120 °C significantly improved the carbonation conversion of 20Ce-CaO-PE-4, with the conversion increasing to 79.6% in the sixth cycle, representing a 45% improvement over the fifth cycle. At 200 and 400 °C, carbonation conversion similarly improved in the sixth cycle, with both temperatures showing higher conversions than in the fifth cycle. However, as the hydration temperature

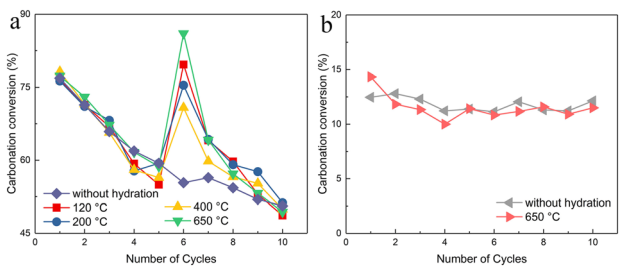

Fig. 8 Reactivity of (a) 20Ce-CaO-PE-4 and (b) CaO-PE-4 hydrated under different temperatures in the dual-packed bed reactor. Reaction conditions: calcination: N_2, 850 °C, 10 min; carbonation: 15% CO_2, 85% N_2, 650 °C, 15 min; hydration: 100% steam, 60 min.

increased from 120 °C to 400 °C, the effect of steam hydration weakened, leading to smaller improvements in carbonation conversion. When the hydration temperature was further increased to 650 °C, the conversion in the sixth cycle increased significantly, surpassing the improvement observed at 120 °C. Despite the initial increase in capacity, the enhanced performance of 20Ce-CaO-PE-4 declined significantly after the sixth cycle, with notable reactivity reduction over the subsequent four cycles. By the tenth cycle, the carbonation conversion approached that of the non-hydrated counterpart, indicating that the positive impact of steam hydration was temporary for these CeO_2-doped CaO-based pellets. Similar findings were also reported by Yu *et al.*,[32] Rong *et al.*,[45,46] and Manovic *et al.*[44] In contrast, steam hydration had little effect on the reactivity of CaO-PE-4, as indicated by the overlapping performance curves across the cycle. This was likely due to the low porosity of CaO-PE-4 after five cycles, with the improvement in porosity from steam hydration in the sixth cycle insufficient to enhance reactivity effectively. This suggested that CeO_2 in the CaO matrix significantly amplified the improvement from steam hydration, highlighting the role of CeO_2 in enhancing its reactivity.

XRD characterization was performed on 20Ce-CaO-PE-4 hydrated at different temperatures (120, 200, 400, and 650 °C) to investigate the structural changes induced by steam hydration. As shown in Fig. S2,† the crystalline phases of 20Ce-CaO-PE-4 after hydration at 120, 200, and 400 °C were identified as CeO_2 and $Ca(OH)_2$, confirming that hydration resulted in the formation of $Ca(OH)_2$. However, hydration at 650 °C resulted in crystalline phases of CeO_2 and CaO, as the hydration reaction (reaction 6) was unfavorable at temperatures above 500 °C.[47,48] SEM analysis (Fig. 9) provided further insight into the structural changes of the hydrated pellets. Significant improvements in pellet porosity were observed after steam hydration, especially at 650 °C, contributing to the increased CO_2 uptake capacity in the sixth cycle. However, increasing the hydration temperature from 120 to 400 °C accelerated the sintering of $Ca(OH)_2$, reducing porosity and decreasing the CO_2 uptake capacity in the sixth cycle. A similar finding was reported by Rong *et al.*, who attributed the reduced effectiveness of steam hydration at 200–500 °C to the sintering effect of $Ca(OH)_2$.[45] While steam hydration resulted in an initial improvement in the porosity of the pellets, sintering continued to occur when the hydrated pellets were subjected to subsequent carbonation/calcination cycles. As a result, the porosity decreased again during cycling, ultimately reaching levels similar to those of the counterparts without hydration (see Fig. 9). Consequently, it seemed that the performance improvement by steam hydration was temporary.

2.4 Effect of steam injection on the reactivity of CeO_2-doped CaO-based pellets

A steam injection strategy was implemented to improve the CO_2 capture performance of CeO_2-doped CaO-based pellets. The pellets were carbonated in 15% CO_2 with varying steam concentrations (*i.e.*, 5%, 10%, 15%, 20%, balanced with N_2)

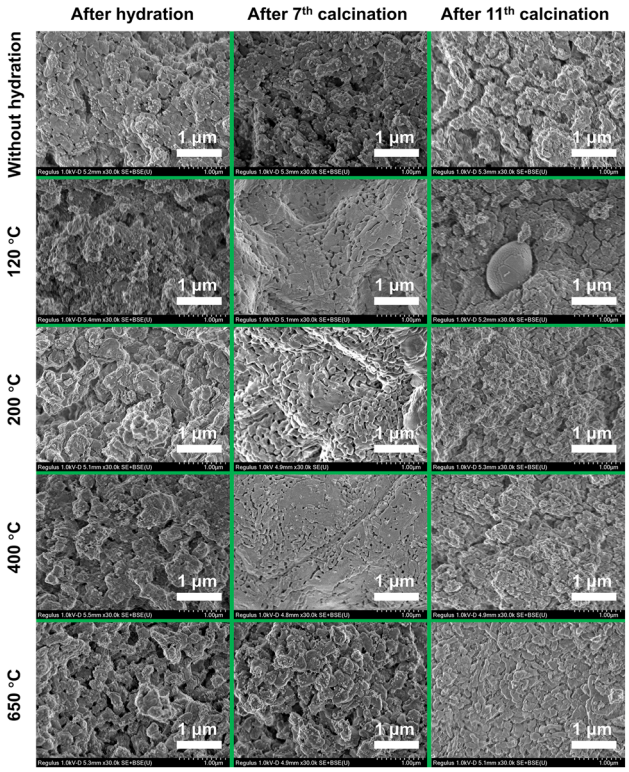

Fig. 9 SEM images of 20Ce-CaO-PE-4 at different hydration temperatures with a hydration duration of 60 min in the dual-packed bed reactor.

in each carbonation reaction, aiming to study the effect of steam injection on their reactivity. As shown in Fig. 10a, introducing 5% steam into the carbonation process did not significantly improve pellet performance compared to the counterpart without steam. The performance curves for pellets with 5% steam and those without steam overlapped almost completely across all cycles. This suggested that at this low steam concentration, steam did not notably alter the reactivity of the pellets. In contrast, increasing the steam concentration to 10% resulted in a noticeable enhancement of carbonation performance. The initial carbonation conversion in the first cycle surged to 93.8%, representing a 22.0% improvement over the counterpart without steam. This

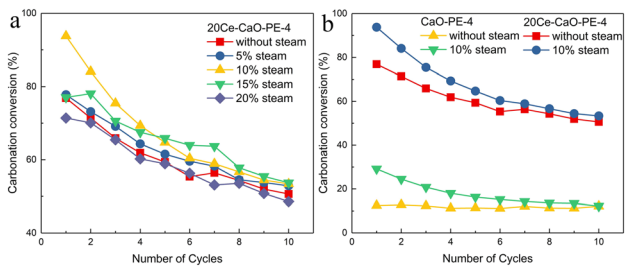

Fig. 10 Reactivity of (a) 20Ce-CaO-PE-4 and (b) CaO-PE-4 at varying concentrations of steam during carbonation in the dual-packed bed reactor. Reaction conditions: calcination: N_2, 850 °C, 10 min; carbonation: 15% CO_2 (balanced with N_2), 650 °C, 15 min.

was due to the catalytic effect of H_2O by forming $Ca(OH)_2$ during the chemical reaction controlled stage, and diffusion enhancement in the $CaCO_3$ product layer mainly during the diffusion controlled stage.[49,50] However, despite the improved initial performance, the reactivity of the pellets declined significantly in the subsequent cycles. By the tenth cycle, the carbonation conversion dropped to 53.4%, slightly higher than the 50.6% conversion observed for pellets without steam, indicating that the effect of steam was not sustained over multiple cycles. This was because the presence of steam during carbonation also promoted the sintering of the sorbents.[51] Further increasing the steam concentration to 15% resulted in a reduction in the carbonation performance compared to the 10% steam condition. The initial carbonation conversion decreased to 77.1%, which, although higher than the counterpart without steam, was lower than that achieved with 10% steam. This implied that while 15% steam offered some performance improvement, it was less effective than 10% steam at sustaining high reactivity across multiple cycles. Finally, introducing 20% steam caused a significant deterioration in carbonation performance. Both initial and final carbonation conversions were much lower than those observed for the counterparts without steam. This indicated that a higher steam concentration had a detrimental effect on the reactivity of the pellets. This was mainly due to that the high steam concentration promoted sintering of the pellets. This result was consistent with previous studies.[51,52]

To further assess the impact of steam injection, a cyclic experiment with 10% steam was conducted on CaO-PE-4. As shown in Fig. 10b, the introduction of 10% steam significantly improved the initial CO_2 capture performance of CaO-PE-4. In the first cycle, the carbonation conversion reached 29.1%, which was 1.34 times higher than that of the counterpart without steam. However, despite this initial boost, a sharp decline in reactivity was observed in subsequent cycles. By the tenth cycle, the carbonation conversion dropped to 12.2%, only slightly higher than the conversion of the counterpart without steam (~12.1%). These results implied that steam injection had a greater effect during the initial cycles for both CeO_2-doped and undoped CaO-based pellets, with the reactivity declining as the cycles progressed. Overall, CeO_2-doped CaO-based pellets consistently outperformed their undoped counterparts, regardless of steam injection. This implied that the presence of CeO_2 in the pellets enhanced their ability to capture CO_2, regardless of the steam concentration. To investigate further, SEM analysis was conducted on spent 20Ce-CaO-PE-4 and spent CaO-PE-4 after ten cycles with steam injection. As shown in Fig. 11, the porosity of spent 20Ce-CaO-PE-4 was significantly higher than that of spent CaO-PE-4. Additionally, both spent 20Ce-CaO-PE-4 and spent CaO-PE-4 exhibited a more porous surface structure compared to their counterparts without steam injection (see Fig. 6f, 9, and 11). This increased porosity was likely responsible for the higher activity observed in the initial cycles, as a more porous surface allowed greater access to CO_2 during carbonation.

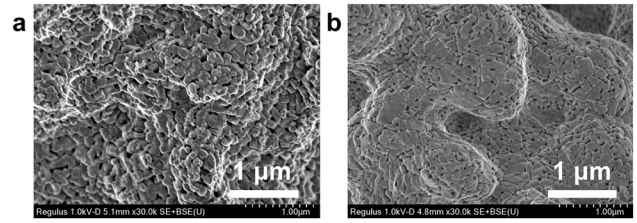

Fig. 11 SEM images of (a) spent 20Ce-CaO-PE-4 and (b) spent CaO-PE-4 after ten cycles in the dual-packed bed reactor. Reaction conditions: calcination: N_2, 850 °C, 10 min; carbonation: 15% CO_2, 10% steam, 75% N_2, 650 °C, 15 min.

3 Conclusions

In this study, powdery CeO_2-doped CaO-based sorbents with varying CeO_2 contents were prepared using the Pechini method. As the CeO_2 content increased from 5 wt% to 20 wt%, the CO_2 capture performance of CeO_2-doped CaO-based sorbents improved significantly. At 20 wt% CeO_2 doping, 20Ce-CaO-PO exhibited the highest initial carbonation conversion of 82.3%, which decreased to 60.1% after ten cycles, preserving 73% of its original reactivity. SEM and TEM analysis confirmed that CeO_2 doping effectively reduced the grain size and mitigated the sintering during cycling. The presence of oxygen vacancies in the CeO_2-doped CaO-based sorbents was confirmed by XPS characterization.

20Ce-CaO-PO was then used to prepare pellets in an industrially relevant form for the first time, with varying particle sizes, including 106–180, 180–250, 250–355, and 355–500 μm. The incorporation of CeO_2 alleviated the negative impact of pelletization and particle size on performance. CeO_2-doped CaO-based pellets with different particle sizes exhibited nearly identical CO_2 capture performance, closely matching the reactivity of powdery CeO_2-doped CaO-based sorbents. The negligible impact of particle size on carbonation performance can be attributed to the slight reduction in the specific surface area and pore volume as the particle size increased. This finding is especially important for industrial applications of CeO_2-doped pellets in fluidized bed systems, where particle size effects on reactivity are a common concern. The reactivity of 20Ce-CaO-PE-4 was further assessed under the industrially relevant calcination conditions. When calcination was performed at 850 °C in steam, 20Ce-CaO-PE-4 had an initial carbonation conversion of 75.1%, which dropped to 29.9% by the 20th cycle, retaining 40% of the original performance.

Furthermore, the effects of two steam-based strategies—steam hydration and steam injection—on the reactivity of the CeO_2-doped pellets were explored. Following the sixth calcination, steam hydration was conducted and significantly improved the reactivity of CeO_2-doped CaO-based pellets. Hydration at 650 °C resulted in a carbonation conversion of 86.0% in the sixth cycle, surpassing the non-hydrated pellets by 55.4%. However, the performance improvement by steam hydration was temporary. Although steam hydration resulted in an initial improvement in the porosity of the pellets, sintering continued to occur when the hydrated pellets were subjected to subsequent carbonation/calcination cycles. As a result, the porosity decreased again during cycling, ultimately reaching levels similar to those of the counterparts without hydration. The effect of steam injection was more complex and highly dependent on the steam concentration. Only a moderate steam concentration (10–15%) enhanced the reactivity, leading to higher carbonation conversions. With 10% steam during carbonation, the initial conversion in the first cycle surged to 93.8%, representing a 22.0% improvement over the counterpart without steam. However, steam injection had a greater effect during the initial cycles, with reactivity declining as the cycles progressed.

4 Experimental

4.1 Synthetic procedures

Powdery CaO-based sorbents were first made using the Pechini method. Specific amounts of $Ca(NO_3)_2{\cdot}4H_2O$, $Ce(NO_3)_3{\cdot}6H_2O$, citric acid, and polyethylene glycol 6000 were dissolved in deionized water. The mixed solution was placed in an electrically heated oil bath at 85 °C and maintained for more than 3 h to obtain a viscous gel. The gel was then transferred to an oven for further drying at 120 °C overnight. The dried sample was carefully ground and calcined in a muffle furnace at 850 °C for 2 h. After calcination, the powdery sample was collected and pelletized into small discs using a manual hydraulic press (DF-4, Gangdong). The pellets were then crushed and sieved to obtain CaO-based pellets with various particle sizes: 106–180 μm, 180–250 μm, 250–355 μm, and 355–500 μm.

For simplicity, *x*Ce-CaO-PO is used to denote powdery CeO_2-doped CaO-based sorbents, where *x* represents the mass fraction of CeO_2. 20Ce-CaO-PE-*Y* denotes CeO_2-doped CaO-based pellets with a 20 wt% CeO_2 mass fraction, where *Y* means the particle size range. Four particle size ranges were prepared: 106–180, 180–250, 250–355, and 355–500 μm, corresponding to *Y* values of 1, 2, 3, and 4, respectively. Additionally, CaO-PO and CaO-PE-4 denote undoped powdery CaO-based sorbents and undoped CaO-based pellets sieved to 355–500 μm, respectively.

4.2 Characterization

Elemental composition was determined using inductively coupled plasma optical emission spectroscopy (ICP-OES, Avio 200). The crystalline phases were analyzed using an X-ray powder diffractometer (XRD, SmartLab). The microstructure and elemental distribution were evaluated using scanning electron microscopy (SEM, Regulus 8100) and transmission electron microscopy (TEM) coupled with energy-dispersive X-ray spectroscopy (EDX). Surface properties were analyzed using an X-ray photoelectron spectrometer (XPS, Nexsa). The specific surface area and pore volume were determined using N_2 physisorption analysis (TriStar II 3020).

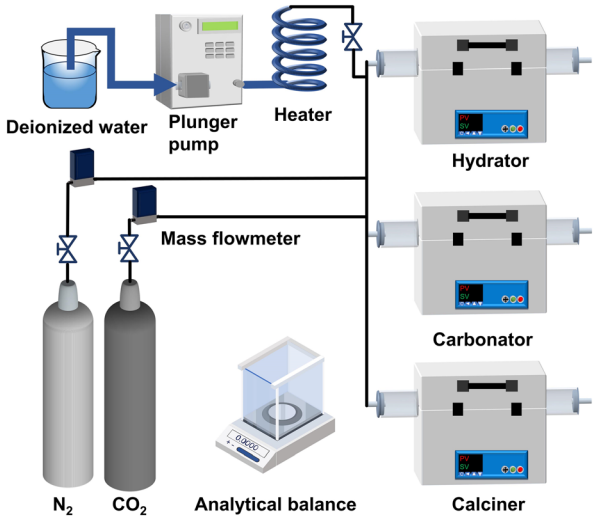

Fig. 12 Diagram of the dual-packed bed reactor.

4.3 Reactivity measurement

The reactivity of sorbents was assessed in a dual-packed bed reactor. As shown in Fig. 12, the dual-packed bed reactor primarily consisted of a hydrator, carbonator, calciner, plunger pump (EPP010S, Elite), heater, gas cylinders (N_2 and CO_2, respectively), and mass flow meters (CS200A, Sevenstar). The plunger pump regulated the flow of deionized water, which was then directed to a heater and vaporized into steam. The sample (~0.15 g) was loaded into a porcelain boat and placed in the calciner. Calcination was carried out at 850 °C for 10 min in N_2 or steam or at 920 °C for 10 min in CO_2. The carbonation reaction was performed at 650 °C for 15 min in 15% CO_2, mixed with varying amounts of steam (balanced with N_2). Steam hydration was conducted at temperatures of 120, 200, 400, and 650 °C for durations ranging from 30 to 240 min in pure steam. To simulate multiple carbonation/calcination cycles, the samples were alternately subjected to the calcination and carbonation reactions. After each reaction, the sample was removed and cooled for 10 min in a dryer. The cooled sample's mass was then measured precisely using an analytical balance (ME104) with a precision of 0.0001 g.

In addition, the CO_2 sorption rate during the carbonation reaction was also investigated in a vertical fixed bed reactor. Details of the setup are described in our previous study.[25] Typically, the carbonation was performed at 650 °C for 15 min in 15% CO_2 (balanced with N_2), while the calcination was conducted at 850 °C for 10 min in N_2. A total gas flow rate of 400 mL min^{-1} was used in each stage. The CO_2 concentration in the off-gas was measured using a gas analyzer.

The carbonation conversion (eqn (1) and (2)) was used to evaluate the performance of sorbents, as defined by the following equations:

$$\text{Carbonation conversion} = \frac{m_{\text{car},N} - m_{\text{cal},N}}{m_{\text{cal},1}\cdot\varphi_{\text{CaO}}}\cdot\frac{56}{44} \quad (1)$$

$$\text{Carbonation conversion} = \frac{\int_0^t \left(c_{\text{CO}_2}^{\text{in}} - c_{\text{CO}_2}^{\text{out}}(t')\right)\mathrm{d}t' \times Q}{22.4 \times \varphi_{\text{CaO}}} \quad (2)$$

where $m_{\text{cal},N}$ is the sample mass after the Nth calcination; $m_{\text{car},N}$ is the sample mass after the Nth carbonation reaction; $m_{\text{cal},1}$ is the sample mass after the first calcination reaction; φ_{CaO} is the CaO content in the sample; $c_{\text{CO}_2}^{\text{in}}$ is the inlet CO_2 concentration; $c_{\text{CO}_2}^{\text{out}}(t')$ is the outlet CO_2 concentration at time t'; and Q denotes the total gas flow rate.

Data availability

The data supporting this article are available within the article and its ESI.† If necessary, the raw data are available upon request to the corresponding author (Dr. Jian Chen and Prof. Lunbo Duan).

Author contributions

Yong Li: methodology, investigation, data curation, and writing – original draft. Wuhao Sun: methodology and investigation. Xilei Liu: methodology and investigation. Hedan Tang: methodology and investigation. Jian Chen: conceptualization, funding acquisition, supervision, and writing – review & editing. Youshi Li: methodology and investigation. Mingdi Li: methodology and investigation. Lunbo Duan: conceptualization, supervision, and writing – review & editing.

Conflicts of interest

There are no conflicts to declare.

Acknowledgements

We acknowledge the financial support from the National Natural Science Foundation of China (No. 52206230) and the Natural Science Research of Jiangsu Higher Education Institutions of China (22KJB480001).

References

1 M. T. Dunstan, F. Donat, A. H. Bork, C. P. Grey and C. R. Müller, CO_2 capture at medium to high temperature using solid oxide-based sorbents: Fundamental aspects, mechanistic insights, and recent advances, *Chem. Rev.*, 2021, **121**, 12681–12745.

2 J. Chen, L. Duan, Y. Ma, Y. Jiang, A. Huang, H. Zhu, H. Jiao, M. Li, Y. Hu, H. Zhou, Y. Xu, F. Donat, M. Awais Naeem and O. Kröcher, Recent progress in calcium looping integrated with chemical looping combustion (CaL-CLC) using bifunctional CaO/CuO composites for CO_2 capture: A state-of-the-art review, *Fuel*, 2023, **334**, 126630.

3 I. Martínez, G. Grasa, J. Parkkinen, T. Tynjälä, T. Hyppänen, R. Murillo and M. C. Romano, Review and research needs of Ca-Looping systems modelling for post-combustion CO_2

capture applications, *Int. J. Greenhouse Gas Control*, 2016, **50**, 271–304.

4 B. Arias, M. E. Diego, A. Méndez, M. Alonso and J. C. Abanades, Calcium looping performance under extreme oxy-fuel combustion conditions in the calciner, *Fuel*, 2018, **222**, 711–717.

5 M. Hornberger, J. Moreno, M. Schmid and G. Scheffknecht, Experimental investigation of the calcination reactor in a tail-end calcium looping configuration for CO_2 capture from cement plants, *Fuel*, 2021, **284**, 118927.

6 H. Sun, C. Wu, B. Shen, X. Zhang, Y. Zhang and J. Huang, Progress in the development and application of CaO-based adsorbents for CO_2 capture—A review, *Mater. Today Sustain.*, 2018, **1–2**, 1–27.

7 J. Chen, L. Duan and Z. Sun, Review on the development of sorbents for calcium looping, *Energy Fuels*, 2020, **34**, 7806–7836.

8 S. M. Hashemi, M. H. Sedghkerdar and N. Mahinpey, Calcium looping carbon capture: Progress and prospects, *Can. J. Chem. Eng.*, 2022, **100**, 2140–2171.

9 J. Chen, A. Huang, C. Huang, W. Xia, H. Tang, C. Liu, Y. Xu, Y. Li, Z. Wang and B. Qian, Stabilizer-coated combined Ca/Cu pellets with controllable particle sizes for the Ca/Cu chemical loop, *Sep. Purif. Technol.*, 2024, **338**, 126535.

10 Y. Hu, H. Lu, W. Liu, Y. Yang and H. Li, Incorporation of CaO into inert supports for enhanced CO_2 capture: A review, *Chem. Eng. J.*, 2020, **396**, 125253.

11 P. Teixeira, C. Bacariza, I. Mohamed and C. I. C. Pinheiro, Improved performance of modified CaO-Al_2O_3 based pellets for CO_2 capture under realistic Ca-looping conditions, *J. CO_2 Util.*, 2022, **61**, 102007.

12 H. J. Yoon and K. B. Lee, Introduction of chemically bonded zirconium oxide in CaO-based high-temperature CO_2 sorbents for enhanced cyclic sorption, *Chem. Eng. J.*, 2019, **355**, 850–857.

13 M. A. Naeem, A. Armutlulu, Q. Imtiaz, F. Donat, R. Schaublin, A. Kierzkowska and C. R. Muller, Optimization of the structural characteristics of CaO and its effective stabilization yield high-capacity CO_2 sorbents, *Nat. Commun.*, 2018, **9**, 2408.

14 D. He, C. Qin, Z. Zhang, S. Pi, J. Ran and G. Pu, Investigation of Y_2O_3/M_xO_y-incorporated Ca-based sorbents for efficient and stable CO_2 capture at high temperature, *Ind. Eng. Chem. Res.*, 2018, **57**, 11625–11635.

15 M. Imani, M. Tahmasebpoor, P. Enrique Sánchez-Jiménez, J. Manuel Valverde and V. Moreno, A novel, green, cost-effective and fluidizable SiO_2-decorated calcium-based adsorbent recovered from eggshell waste for the CO_2 capture process, *Sep. Purif. Technol.*, 2023, **305**, 122523.

16 M. Krödel, L. Abduly, M. Nadjafi, A. Kierzkowska, A. Yakimov, A. H. Bork, F. Donat, C. Copéret, P. M. Abdala and C. R. Müller, Structure of Na species in promoted CaO-based sorbents and their effect on the rate and extent of the CO_2 uptake, *Adv. Funct. Mater.*, 2023, **33**, 2302916.

17 D. Choi, A.-H. Alissa Park and Y. Park, Effects of eutectic alkali chloride salts on the carbonation reaction of CaO-based composites for potential application to a thermochemical energy storage system, *Chem. Eng. J.*, 2022, **437**, 135481.

18 Y. Xu, F. Donat, C. Luo, J. Chen, A. Kierzkowska, M. Awais Naeem, L. Zhang and C. R. Müller, Investigation of K_2CO_3-modified CaO sorbents for CO_2 capture using in-situ X-ray diffraction, *Chem. Eng. J.*, 2023, **453**, 139913.

19 X. Yan, C. Duan, S. Yu, B. Dai, C. Sun and H. Chu, Revealing the mechanism of oxygen vacancy defect for CO2 adsorption and diffusion on CaO: DFT and experimental study, *J. CO2 Util.*, 2024, **79**, 102648.

20 K. B. Yi, C. H. Ko, J.-H. Park and J.-N. Kim, Improvement of the cyclic stability of high temperature CO_2 absorbent by the addition of oxygen vacancy possessing material, *Catal. Today*, 2009, **146**, 241–247.

21 Z. Yuyuan, G. Zhiwei, S. Haocheng, W. Liang, Z. Shuang, L. Xipeng, C. Qicheng and C. Haisheng, The role of oxygen vacancy in CaO-$Ca_{12}Al_{14}O_{33}$ materials derived from hydrocalumite for enhanced CO_2 capture cyclic performance, *Chem. Eng. J.*, 2024, **481**, 147955.

22 S. Wang, S. Fan, L. Fan, Y. Zhao and X. Ma, Effect of cerium oxide doping on the performance of CaO-based sorbents during calcium looping cycles, *Environ. Sci. Technol.*, 2015, **49**, 5021–5027.

23 H. Guo, X. Kou, Y. Zhao, S. Wang and X. Ma, Role of microstructure, electron transfer, and coordination state in the CO_2 capture of calcium-based sorbent by doping (Zr-Mn), *Chem. Eng. J.*, 2018, **336**, 376–385.

24 X. Liu, J. Chen, Y. Ma, C. Liu, A. Huang, J. He, M. Wang, H. Tang, W. Zuo and Y. Li, Synergistic effects of CeO_2 and Al_2O_3 on reactivity of CaO-based sorbents for CO_2 capture, *Sep. Purif. Technol.*, 2024, **347**, 127660.

25 Y. Jiang, J. Chen, F. Chen, M. Wang, Y. Li, M. Li, B. Qian, Z. Wang, S. Zhang and H. Zhou, Synergistic enhancement of Ca-based materials via CeO_2 and Al_2O_3 co-doping for enhanced CO_2 capture and thermochemical energy storage in calcium looping technology, *Sep. Purif. Technol.*, 2025, **358**, 130264.

26 I. Yanase, T. Maeda and H. Kobayashi, The effect of addition of a large amount of CeO_2 on the CO_2 adsorption properties of CaO powder, *Chem. Eng. J.*, 2017, **327**, 548–554.

27 X. Yan, Y. Li, X. Ma, Z. Bian, J. Zhao and Z. Wang, CeO_2-modified CaO/$Ca_{12}Al_{14}O_{33}$ bi-functional material for CO_2 capture and H_2 production in sorption-enhanced steam gasification of biomass, *Energy*, 2020, **192**, 116664.

28 H. Guo, J. Feng, Y. Zhao, S. Wang and X. Ma, Effect of micro-structure and oxygen vacancy on the stability of (Zr-Ce)-additive CaO-based sorbent in CO_2 adsorption, *J. CO_2 Util.*, 2017, **19**, 165–176.

29 J. Dong, Y. Tang, A. Nzihou and E. Weiss-Hortala, Effect of steam addition during carbonation, calcination or hydration on re-activation of CaO sorbent for CO_2 capture, *J. CO_2 Util.*, 2020, **39**, 101167.

30 L. Chen and N. Qian, The effects of water vapor and coal ash on the carbonation behavior of CaO-sorbent supported by γ-Al_2O_3 for CO_2 capture, *Fuel Process. Technol.*, 2018, **177**, 200–209.

31 V. Manovic, P. S. Fennell, M. J. Al-Jeboori and E. J. Anthony, Steam-enhanced calcium looping cycles with calcium aluminate pellets doped with bromides, *Ind. Eng. Chem. Res.*, 2013, **52**, 7677–7683.

32 Z. Yu, L. Duan, C. Su, Y. Li and E. J. Anthony, Effect of steam hydration on reactivity and strength of cement-supported calcium sorbents for CO_2 capture, *Greenhouse Gases:Sci. Technol.*, 2017, **7**, 915–926.

33 S. Zhang, L. Zhang and F. Duan, Sulfation, pore, and fractal properties of hydrated spent calcium magnesium acetate from calcium-based looping, *Greenhouse Gases:Sci. Technol.*, 2019, **9**, 539–552.

34 L. Zhang, B. Zhang, Z. Yang and M. Guo, The role of water on the performance of calcium oxide-based sorbents for carbon dioxide capture: A review, *Energy Technol.*, 2014, **3**, 10–19.

35 Y. Long, J. Sun, C. Mo, X. She, P. Zeng, H. Xia, J. Zhang, Z. Zhou, X. Nie and C. Zhao, One-step fabricated Zr-supported, CaO-based pellets via graphite-moulding method for regenerable CO_2 capture, *Sci. Total Environ.*, 2022, **851**, 158357.

36 J. Chen, Y. Jiang, X. Liu, W. Xia, A. Huang, J. Zong, Z. Wang, B. Qian and F. Donat, One-step synthesis of CaO/CuO composite pellets for enhanced CO_2 capture performance in a combined Ca/Cu looping process via a facile gel-casting technique, *Sep. Purif. Technol.*, 2024, **328**, 125057.

37 J. Phanthasri, T. Saelee, N. Sosa, S. Youngjan, N. Samart, M. Rittiruam, P. Khajondetchairit, S. Chomchin, T. Chankhanittha, K. Prasitnok, S. Kiatphuengporn, M. Chareonpanich, N. Chanlek, S. Nijpanich, P. Kidkhunthod, P. Praserthdam, S. Praserthdam and P. Khemthong, Integrated experimental and theoretical studies for unravelling CO_2 capture of dual function CeO_2-CaO bio-based sorbents, *J. Environ. Chem. Eng.*, 2024, **12**, 112412.

38 J. Lin, W. Kong, C. Qiu, X. Zhong, Y. Li, M. Fu and Z. Li, New insight into catalytic performance and reaction mechanism for butyl acetate over CeO_2 catalysts: Oxygen vacancy and surface reactive oxygen species, *J. Environ. Chem. Eng.*, 2024, **12**, 114046.

39 S. Wu, H. Liu, Z. Huang, H. Xu and W. Shen, $Mn_1Zr_xO_y$ mixed oxides with abundant oxygen vacancies for propane catalytic oxidation: Insights into the contribution of Zr doping, *Chem. Eng. J.*, 2023, **452**, 139341.

40 J. Sun, W. Liu, Y. Hu, J. Wu, M. Li, X. Yang, W. Wang and M. Xu, Enhanced performance of extruded-spheronized carbide slag pellets for high temperature CO_2 capture, *Chem. Eng. J.*, 2016, **285**, 293–303.

41 C. Qin, H. Du, L. Liu, J. Yin and B. Feng, CO_2 capture performance and attrition property of CaO-based pellets manufactured from organometallic calcium precursors by extrusion, *Energy Fuels*, 2013, **28**, 329–339.

42 F. N. Ridha, V. Manovic, A. Macchi and E. J. Anthony, High-temperature CO_2 capture cycles for CaO-based pellets with kaolin-based binders, *Int. J. Greenhouse Gas Control*, 2012, **6**, 164–170.

43 Y. Wu, V. Manovic, I. He and E. J. Anthony, Modified lime-based pellet sorbents for high-temperature CO_2 capture: Reactivity and attrition behavior, *Fuel*, 2012, **96**, 454–461.

44 V. Manovic and E. J. Anthony, Reactivation and remaking of calcium aluminate pellets for CO_2 capture, *Fuel*, 2011, **90**, 233–239.

45 N. Rong, Q. Wang, M. Fang, L. Cheng, Z. Luo and K. Cen, Steam hydration reactivation of CaO-based sorbent in cyclic carbonation/calcination for CO_2 capture, *Energy Fuels*, 2013, **27**, 5332–5340.

46 N. Rong, Y. Wu, J. Wang, L. Han and G. Wang, Steam reactivation of biotemplated CaO-based pellets for cyclic CO_2 capture, *Energy Fuels*, 2021, **35**, 6056–6067.

47 K. Wang, T. Yan, R. K. Li and W. G. Pan, A review for $Ca(OH)_2$/CaO thermochemical energy storage systems, *J. Energy Storage*, 2022, **50**, 104612.

48 S. Funayama, H. Takasu, S. T. Kim and Y. Kato, Thermochemical storage performance of a packed bed of calcium hydroxide composite with a silicon-based ceramic honeycomb support, *Energy*, 2020, **201**, 117673.

49 S. Yang and Y. Xiao, Steam catalysis in CaO carbonation under low steam partial pressure, *Ind. Eng. Chem. Res.*, 2008, **47**, 4043–4048.

50 V. Manovic and E. J. Anthony, Carbonation of CaO-based sorbents enhanced by steam addition, *Ind. Eng. Chem. Res.*, 2010, **49**, 9105–9110.

51 C. Li, C. Zhang and X. Guo, Sintering mechanism of CaO during carbonation reaction in the presence of water vapor, *Proc. Combust. Inst.*, 2023, **39**, 4467–4476.

52 Z. He, Y. Li, X. Ma, W. Zhang, C. Chi and Z. Wang, Influence of steam in carbonation stage on CO_2 capture by Ca-based industrial waste during calcium looping cycles, *Int. J. Hydrogen Energy*, 2016, **41**, 4296–4304.